Photosynth Res (2017) 133:103–114
DOI 10.1007/s11120-017-0349-z

ORIGINAL ARTICLE

Connectivity between electron transport complexes and modulation of photosystem II activity in chloroplasts

Alexander N. Tikhonov[1] · **Alexey V. Vershubskii**[1]

Received: 9 December 2016 / Accepted: 2 February 2017 / Published online: 8 March 2017

Abstract In chloroplasts, photosynthetic electron transport complexes interact with each other via the mobile electron carriers (plastoquinone and plastocyanin) which are in surplus amounts with respect to photosystem I and photosystem II (PSI and PSII), and the cytochrome b_6f complex. In this work, we analyze experimental data on the light-induced redox transients of photoreaction center P_{700} in chloroplasts within the framework of our mathematical model. This analysis suggests that during the action of a strong actinic light, even significant attenuation of PSII [for instance, in the result of inhibition of a part of PSII complexes by DCMU or due to non-photochemical quenching (NPQ)] will not cause drastic shortage of electron flow through PSI. This can be explained by "electronic" and/or "excitonic" connectivity between different PSII units. At strong AL, the overall flux of electrons between PSII and PSI will maintain at a high level even with the attenuation of PSII activity, provided the rate-limiting step of electron transfer is beyond the stage of PQH_2 formation. Results of our study are briefly discussed in the context of NPQ-dependent mechanism of chloroplast protection against light stress.

Keywords Chloroplasts · Electron transport · Proton potential · Interaction of electron transport complexes · Mathematical modeling

The original version of this article has been revised: The figure part labels in Fig. 5 have been corrected.

✉ Alexander N. Tikhonov
an_tikhonov@mail.ru; an_tikhonov@physics.msu.ru

[1] Faculty of Physics, Moscow State University, Moscow, Russia 119991

Abbreviations

AL	Actinic light
b_6f	Cytochrome b_6f complex
CBC	Calvin–Benson cycle
Chl	Chlorophyll
DCMU	3-(3,4-Dichlorophenyl)-1,1′-dimethylurea
EPR	Electron paramagnetic resonance
ETC	Electron transport chain
Fd	Ferredoxin
FNR	Ferredoxin-NADP-oxidoreductase
HL, HAL	High light, high actinic light,
LL, LAL	Low light, low actinic light
LHCII	Light-harvesting complex II
MV	Methyl viologen
NPQ	Non-photochemical quenching
pmf	Proton motive force
PSA	Photosynthetic apparatus
PSI	Photosystem I
PSII	Photosystem II
P_{700}, P^+_{700}	Reduced and oxidized forms of primary electron donor in PSI, respectively
P_{680}, P^+_{680}	Reduced and oxidized forms of primary electron donor in PSII, respectively
Pc	Plastocyanin
PQ	Plastoquinone
PQ_A	Primary plastoquinone bound to PSII
PQ_B	Secondary plastoquinone bound to PSII
PQH_2	Plastoquinol
ROS	Reactive oxygen species
S_0, S_1, S_2, S_3	Long-lived states of the water-oxidizing complex
Tyr_Z	Electron donor for P^+_{680}
WL	White light
WOC	Water-oxidizing complex

WWC	Water–water cycle
ΔpH	*Trans*-thylakoid pH difference

Introduction

Oxygenic photosynthesis is one of the most important processes in Biosphere, which provides the light-induced consumption of carbon dioxide and regeneration of molecular oxygen. Photosynthetic apparatus (PSA) of oxygenic organisms (plants, algae, and cyanobacteria) contains two protein-pigment complexes, Photosystem I (PSI) and Photosystem II (PSII), driving electrons from the water-oxidizing complex (WOC) of PSII to the terminal electron acceptor of PSI, $NADP^+$ (Blankenship 2002; Eberhard et al. 2008; Nelson and Cox 2012; Mamedov et al. 2015). PSI and PSII are interconnected via the cytochrome (Cyt) b_6f complex and mobile electron carriers, plastoquinone (PQ) and plastocyanin (Pc). The rate-limiting step of electron transfer in the chain between PSII and PSI is associated with plastoquinol (PQH_2) oxidation by the Cyt b_6f complex (Stiehl and Witt 1969; Witt 1979; Haehnel 1982, 1984). Under the normal physiological conditions, the light-induced reduction of PQ to PQH_2 in PSII and PQH_2 diffusion within the thylakoid membrane occur more rapidly ($t_{1/2} \leq 2$–5 ms) than PQH_2 oxidation by the Cyt b_6f complexes ($t_{1/2} \geq 5$–20 ms) (for review, see Haehnel 1976; Tikhonov 2013, 2014, 2015). Electron transport through the intersystem electron transport chain (ETC) is coupled to acidification of the thylakoid lumen and alkalization of stroma, thereby generating the *trans*-thylakoid difference in electrochemical potentials of protons ($\Delta\tilde{\mu}_{H^+}$), which serves as the driving force for ATP synthesis (Mitchell 1966; Junge and Nelson 2015). ATP and NADPH are used mainly in biosynthetic processes of the Calvin–Benson cycle (CBC) (Edwards and Walker 1983).

Molecular mechanisms of functioning and structural properties of PSA are currently studied in sufficient details at different levels of its organization. However, the problem of optimal functioning of photosynthetic systems remains in the focus of numerous works in the field (for reference, see Eberhard et al. 2008; Horton 2012; Ruban 2012). In nature, photosynthetic organisms are subjected to variable environmental light, intensity of which spans in a wide range. Rapid fluctuations and excess light are the hazardous factors that may cause damage to PSA (Tikkanen et al. 2012; Yamamoto and Yoshioka-Nishimura 2016). There are several mechanisms of electron transport control providing a well-balanced performance of PSA and its protection against light stress (Allakhverdiev and Murata 2004; Li et al. 2009; Murata et al. 2012; Ruban 2012; Schmitt et al. 2014; Jallet et al. 2016). Photoprotective response of PSA to excessive light develops ranging from a few to dozens of minutes (Demmig-Adams et al. 2012; Jallet et al. 2016). One of the most important mechanisms of photoprotection is associated with the non-photochemical quenching (NPQ) of pigment excitation in the light-harvesting antennae of PSII. NPQ enhances dissipation of excess light energy to heat, thereby diminishing the hazard of PSA damage by aggressive species, e.g., singlet oxygen $^1O_2$, superoxide radicals, and other forms of reactive oxygen species (ROS). In plants, the mechanism of NPQ generation is triggered by the light-induced acidification of the thylakoid lumen. There are two basic events of NPQ induction: protonation of the regulatory protein of PSII, PsbS (Li et al. 2000, 2002, 2004), and conversion of violaxanthin to zeaxanthin (Demmig-Adams 1990; Jahns and Holzwarth 2012; Horton 2012; Ruban et al. 2012). Generation of NPQ attenuates the overall activity of PSII, thereby precluding the formation of ROS caused by side reactions of electron transfer upon the "traffic jam" in the ETC segment beyond PSII. State transitions, associated with the redistribution of absorbed light quanta between PSII and PSI (Horton 2012; Tikkanen and Aro 2012, 2014; Lemeille and Rochaix 2010; Tikkanen et al. 2012; Rochaix 2014), and redistribution of electron fluxes between alternative pathways (Michelet et al. 2013; Balsera et al. 2016; Puthiyaveetil et al. 2016) represent other regulatory mechanisms in chloroplasts.

The capability of plants to resist solar stress by the development of NPQ depends on the growth conditions and plant species (Demmig-Adams et al. 2012; Matsubara et al. 2012; Ocampo-Alvarez et al. 2013; Ware et al. 2015a). Acclimation of plants to high light (HL) enhances the expression of the regulatory protein PsbS (Ballottari et al. 2007; Ware et al. 2015b; Mishanin et al. 2016). PsbS causes the remodeling of the PSII–LHCII supercomplex under elevated light conditions (Johnson et al. 2011; Ruban 2012; Ikeuchi et al. 2014; Dong et al. 2015). In the context of NPQ-dependent regulation of electron transport in chloroplasts, the question arises: how a decrease in the activity of PSII caused by NPQ will reveal itself in the overall flow of electrons from PSII to PSI? In our previous works (Mishanin et al. 2016, 2017), we demonstrated that the long-term acclimation of *Tradescantia* plants to HL growth conditions facilitated the development of high NPQ at strong AL, whereas a steady-state level of P^+_{700} was virtually independent of growth light. In this work, by analyzing experimental and theoretical data on the redox transients of P_{700}, we conclude that even significant attenuation of PSII activity during the action of strong AL should not cause dramatic shortage of electron flow through PSI. This can be explained by "excitonic" and "electronic" connectivity of PSII units, which provide sustainable operation of the chloroplast ETC during the excess of AL. Results of our study are briefly discussed in the context of NPQ-dependent mechanism of PSA protection against the light stress.

Materials and methods

Chloroplasts

Class B chloroplasts were isolated from bean leaves as described earlier (Tikhonov and Ruuge 1979; Tikhonov et al. 1981). Chloroplasts (1–2 mg Chl/ml) were suspended in the media containing 2 mM $MgCl_2$, 200 mM sucrose, and 5 mM Tricine buffer (pH 7.5). These preparations of chloroplasts were able to synthesize ATP because they maintained the integrity of their thylakoids (Tikhonov et al. 1981). Methyl viologen (20 μM) was added as the artificial mediator of electron transfer from PSI to O_2. Chloroplasts were illuminated by the far-red light ($\lambda_{max}=707$ nm, $\Delta\lambda_{1/2}=5$ nm) exciting predominantly PSI or by the orange light ($\lambda_{max}=600$ nm, $\Delta\lambda_{1/2}=7$ nm) exciting the light-harvesting antennas of both PSI and PSII. The far-red (λ_{707}) and orange (λ_{600}) bands of AL were selected from the white light produced by the incandescent lamp using the interference filters SIF707 and SIF600 (Carl Zeiss Jena, Germany). Maximal intensities of the far-red light λ_{707} and the orange light λ_{600} were equal to 75 μmol m^{-2} s^{-1}. Saturating pulses of white light ($t_{1/2}=7$ μs) were produced by a xenon lamp as described in (Tikhonov and Ruuge 1979). The duration of pulses was sufficiently short to provide a single operation of PSII reaction centers. EPR spectra of cation radicals P^+_{700} (Webber and Lubitz 2001) were taken with X-band EPR spectrometer E-4 (Varian, USA) as described in (Tikhonov et al. 1981).

Mathematical model of electron transport in chloroplasts

Computer modeling of photosynthetic processes provides an efficient means for numerical analysis of electron and proton transport in chloroplasts (for recent reviews, see Riznichenko and Rubin 2014; Tikhonov 2016). Figure 1 depicts the diagram of electron and proton transport processes considered in this work within the frames of our mathematical model (Vershubskii et al. 2001, 2004, 2011, 2017; Tikhonov and Vershubskii 2014; Tikhonov 2016). The model describes the key stages of electron transfer from the WOC of PSII to external electron acceptors of PSI ($H_2O \rightarrow$ PSII $\rightarrow$ PQ $\rightarrow$ $b_6f \rightarrow$ Pc $\rightarrow$ PSI $\rightarrow$ CBC/O_2). Mobile electron carriers, plastoquinone (PQ) and plastocyanin (Pc), mediate electron transfer between PSII and PSI. Reduced plastoquinone molecules (plastoquinol, PQH_2), diffusing in the thylakoid

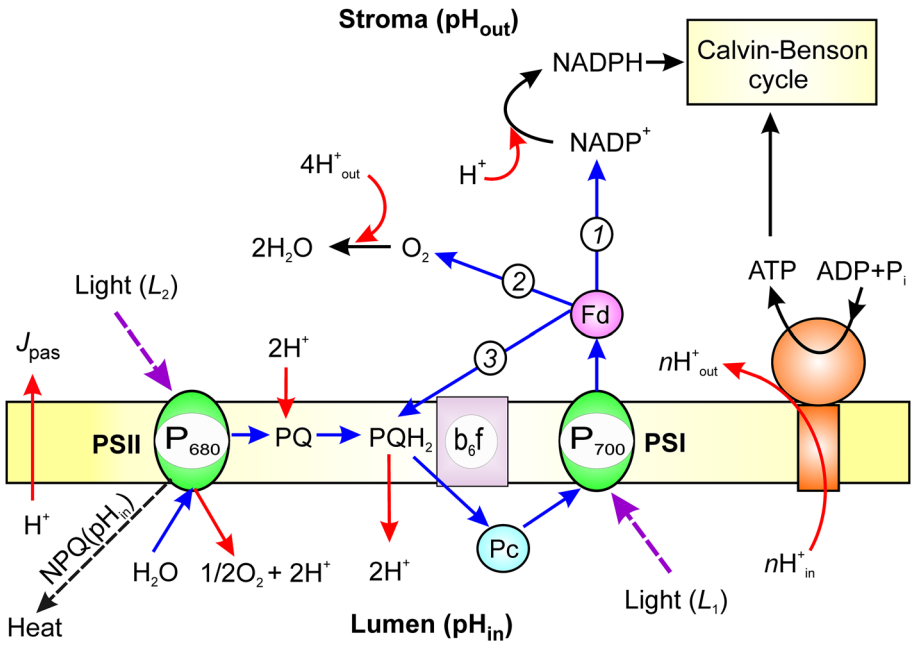

Fig. 1 A scheme of electron transfer and proton transport processes considered in the model and the arrangement of protein complexes (PSI, PSII, the Cyt b_6f, and the ATP synthase complexes) in the thylakoid membrane. Two electrons extracted from the water molecule in PSII are used to reduce PQ to PQH_2. Electrons from PQH_2 are transferred through the cytochrome b_6f complex to reduce plastocyanin (Pc). PSI oxidizes Pc on the lumenal side of the thylakoid membrane and reduces a mobile electron carrier ferredoxin (Fd) on the stromal side of the membrane. Reduced Fd molecules pass electrons to $NADP^+$ (*pathway 1*). Reduced NADPH molecules and ATP are consumed in the Calvin–Benson cycle. Along with the linear electron flow from H_2O to $NADP^+$, the model takes into account alternative routes of electron transport: electron transfer from PSI to O_2 (the Mehler reaction, *pathway 2*), and cyclic electron transport around PSI (*pathway 3*). The *trans*-thylakoid proton transport processes (shown by *red arrows*) coupled to the light-induced electron transport reactions (shown by *blue arrows*) provide generation of ΔpH. For true colors, see the online version of this article

membrane, connect electronically PSII complexes with the Cyt b_6f complex. PQH_2 oxidation by the Cyt b_6f complex is the rate-limiting step in the intersystem chain of electron transport. We take into account that the rate of PQH_2 oxidation depends on the *intra*-thylakoid pH (pH_{in}), because this process is coupled to proton dissociation into the lumen ($PQH_2 \rightarrow PQ + 2H^+_{in} + 2e^-$). Pc diffuses within the thylakoid lumen, providing electron transfer from the Cyt b_6f complexes to PSI. On the acceptor side of PSI, we consider three alternative pathways of electron outflow form PSI: (1) electron drain to $NADP^+$ ($NADP^+ + 2e^- + H^+_{out} \rightarrow NADPH$) and consumption of NADPH in the Calvin–Benson cycle (CBC), (2) electron transfer to O_2 (Mehler 1951; Asada 1999), and (3) a "short" pathway of cyclic electron transfer around PSI (Strand et al. 2016).

We also take into account the proton transport processes leading to generation of the *trans*-thylakoid pH difference, $\Delta pH = pH_{out} - pH_{in}$. The ΔpH-driven ATP synthesis from ADP and P_i was calculated as described earlier (Vershubskii et al. 2001, 2004, 2011, 2017). NADPH and ATP molecules are consumed in the CBC. The light-induced activation of the CBC depends on the stromal pH (pH_{out}) as it was described in (Kuvykin et al. 2009).

The model parameters L_1 and L_2 characterize the relative numbers of absorbed light quanta which actuate the operation of PSI and PSII, respectively. For modeling the action of the far-red light, which excites predominantly PSI ("Light 1"), we have taken the ratio $L_1/L_2 = 16$. For simulation of the AL efficiently exciting both PSI and PSII ("Light 2"), we have used the ratio $L_1/L_2 = 0.7$. These values of L_1/L_2 are consistent with the action spectra of PSI and PSII reported for leaves of different species in (Boichenko 1998; Laisk et al. 2014). We also take into account the light-induced decrease in photochemical activity of PSII caused by acidification of the lumen, which simulates the generation of NPQ in intact chloroplasts (Kuvykin et al. 2011; Trubitsin et al. 2015). Other details of modeling electron and proton transport, including the choice of rate constants and basic parameters of the model, were described in our previous works (Vershubskii et al. 2001, 2004, 2011). For simulation of the inhibitory action of DCMU on PSII activity, we attenuated the model parameter k_{P680}, value of which determines an apparent rate constant of the light-induced electron transfer from P_{680} to the PQ pool (Vershubskii et al. 2004, 2011). In the meantime, upon the reduction of the model parameter k_{P680} (in order to simulate the action of DCMU), we retain the values of the model parameters L_1 and L_2, which determine the frequencies of excitation of PSI and PSII reaction centers.

Results and discussion

Experimental data

In this section, we analyze our experimental data obtained for class B chloroplasts (often termed as thylakoids), which provide a simple model for quantitative analysis of connectivity between the intersystem ETCs. In class B chloroplasts, the CBC reactions and the cyclic route of electron flow around PSI are inefficient because of the losses of ferredoxin and CBC enzymes (soluble proteins). In aerated thylakoids, the photosynthetic ETC operates as the chain of pseudocyclic electron transfer, often termed as the water–water cycle (WWC): $H_2O \rightarrow$ PSII $\rightarrow$ PQ $\rightarrow b_6f \rightarrow$ Pc $\rightarrow$ PSI $\rightarrow O_2 \rightarrow H_2O$ (Mehler 1951; Asada 1999; Miyake 2010). The WWC includes the reaction of O_2 reduction by PSI. Methyl viologen (MV), the artificial mediator of electron transfer added to chloroplasts, promotes the reduction of O_2 by isolated PSI complexes (Kozuleva et al. 2014; Trubitsin et al. 2014) and electron transfer to O_2 in intact chloroplasts in situ (Trubitsin et al. 2015). Note that in aerated chloroplasts, the overall rate of MV-mediated electron flow (PSI $\rightarrow$ MV $\rightarrow O_2$) does not limit the operation of the WWC chain (for the proof of this statement, see Appendix).

Reduction of P^+_{700} in response to short single flashes

Figure 2 shows the time-courses of the light-induced redox transients of P_{700} in aerated suspension of dark-adapted bean chloroplasts. Redox transients of P_{700} were monitored by measuring an intensity of the EPR signal I from P^+_{700} as described earlier (Tikhonov and Ruuge 1979; Tikhonov et al. 1981). Illumination of chloroplasts by the far-red light (λ_{707}), absorbed predominantly by PSI, induced oxidation of P_{700}. After ceasing the far-red light, P^+_{700} reduced slowly ($t_{1/2} \approx 30$ s), demonstrating that the pool of electron carriers between PSII and PSI was kept oxidized upon the far-red light illumination. Application of short ($t_{1/2} = 7$ μs) saturating pulses of white light against the background light λ_{707} produced rapid reduction of P^+_{700} due to the injection of electrons from PSII to the intersystem ETC. The drop of P^+_{700} was followed by the re-oxidation of P_{700} due to the action of the far-red light exciting predominantly PSI.

The response of P^+_{700} to a single short flash can be characterized by parameter $\alpha = \Delta P/P$, where ΔP is the drop of the EPR signal from P^+_{700} of amplitude P (see Fig. 2 for definition). We used parameter α as a measure of photochemically active PSII complexes. There are good reasons to believe that each PSII donates one electron (on an average) in response to one short ($t_{1/2} \approx 7$ μs) flash of light. Actually, analyzing charge separation processes in PSII, Cardona et al. (2012) concluded that "within 1 ms the Mn_4Ca cluster

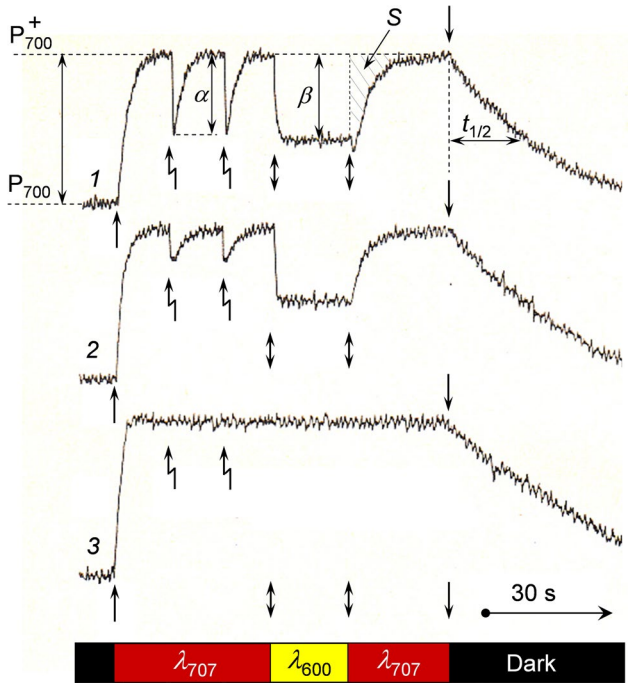

Fig. 2 Time-courses of the light-induced changes in the amplitude of the EPR signal from P^+_{700} in aerated suspension of bean chloroplasts. *Zig-zag arrows* indicate the moments of flashing the short pulses of light. Intensities of continuous actinic light were 37 μmol photons m^{-2} s^{-1} (λ_{707}) and 30 μmol photons m^{-2} s^{-1} (λ_{600}), respectively. *Curve 1*—without added DCMU, *curve 2*—in the presence of 4 μM DCMU, *curve 3*—in the presence of 6.4 μM DCMU

is oxidized by one electron and the quinone is reduced by one electron." A chain of pulse-induced events in PSII of dark-adapted (or far-red light-adapted) chloroplasts is shown below:

$$S_1Tyr_ZP_{680}PQ_APQ_B \xrightarrow{\text{Light}} S_1Tyr_ZP^*_{680}PQ_APQ_B$$
$$\xrightarrow{\approx 200\text{ps}} S_1Tyr_ZP^+_{680}PQ^-_APQ_B \xrightarrow{\approx 20\text{-}40\text{ns}} S_1Tyr^+_ZP_{680}PQ^-_APQ_B$$
$$\xrightarrow{0.2\text{-}0.4\text{ms}} S_1Tyr^+_ZP_{680}PQ_APQ^-_B \xrightarrow{1\text{ms}} S_2Tyr_ZP_{680}PQ_APQ^-_B.$$

This simplified scheme supposes that in dark-adapted (or far-red light-adapted) chloroplasts, the majority of PSII centers are in the S_1PQ_B state (Cardona et al. 2012). In the result of one-electron actuation of PSII, the state $S_2PQ^-_B$ is formed. Here, S_1 and S_2 are the long-lived states of the WOC. After successive donation of the second electron to PQ^-_B, the plastoquinol molecule $(PQH_2)_B$ is formed and then dissociates from PSII ($PQ^-_APQ^-_B \rightarrow PQ_APQ^=_B + 2H^+_{out} \rightarrow PQ_A(PQH_2)_B \rightarrow PQ_A + PQH_2$). Free PQH_2 molecule diffuses toward the Cyt b_6f complex, providing the intersystem electron transport (PSII $\rightarrow PQH_2 \rightarrow b_6f \rightarrow$ Pc $\rightarrow$ PSI).

The reduction of P^+_{700} by ≈50% in response to a single saturating light pulse (Fig. 2, curve 1) can be explained by several reasons. First of all, it is necessary to mention that the yield of PQH_2 per one flash in dark-adapted (or far-red adapted) chloroplasts may reflect the redox state of the acceptor side of PSII. Reduced secondary quinone PQ^-_B decays by charge recombination only when the states S_2 and S_3 are present (Rutherford et al. 1982). State $S_2PQ^-_B$ is relatively stable and decays with a $t_{1/2} \approx 30$ s at 20 °C (Cardona et al. 2012). Populations of PQ^-_B and the long-lived S states (S_0, S_1, S_2, S_3) will determine the yield of PQH_2 per a single flash. Alternative explanation of the reduction of ≈50% centers P^+_{700} per one flash was suggested by Tikhonov and Ruuge (1979) who considered the possibility of cooperation of two adjacent PSII complexes ($2PQ^-_B + 2H^+_{out} \rightarrow (PQH_2)_B + PQ_B$). Also, one cannot exclude that back reactions (e.g., $P^+_{680}PQ^-_A \xrightarrow{0.2\text{ms}} P_{680}PQ_A$) can influence the yield of PQH_2 per flash. In any event, parameter α serves as a measure of a number of active PSII centers capable of donating electrons into the intersystem ETC. The conclusive evidence in favor of this point follows from the results of chloroplast titration with DCMU, the inhibitor of PSII which blocks electron flow from PQ^-_A to the secondary quinone PQ_B. Actually, Fig. 3a shows that parameter α decreases proportionally to concentration of DCMU added to chloroplasts, i.e., α decreases linearly with gradual inactivation of PSII centers.

Reduction of P^+_{700} in response to continuous actinic light

Change-over of the far-red light λ_{707} to continuous orange light ($\lambda_{max} = 600$ nm, $\Delta\lambda_{1/2} = 7$ nm), absorbed by the light-harvesting pigments of both photosystems, induced a decrease in the level of P^+_{700} due to the inflow of electrons to P^+_{700} from PSII via the chloroplast ETC. The drop of P^+_{700} observed after the chromatic transition $\lambda_{707} \rightarrow \lambda_{600}$ we will characterize by parameter β (Fig. 2). Parameter β reflects the capability of PSII for donation of electrons to the intersystem ETC and further to P^+_{700}. Fig. 3a shows that the pattern of the plot of parameter β versus the DCMU concentration markedly differs from the linear law: chloroplasts retain the capability of reducing P^+_{700} upon the illumination by the continuous light λ_{600} even after the inhibition of a substantial portion of PSII complexes. Panel B in Fig. 3 presents the plot of β/β_0 versus α/α_0 (depicted by solid circles with vertical and horizontal bars), where α_0 and β_0 stand for the corresponding parameters determined in control (untreated) chloroplasts, parameters α and β are the corresponding parameters measured in DCMU-treated chloroplasts. This plot demonstrates how a stepwise knockout of PSII centers by DCMU influenced the capacity of PSII for electron donation to the intersystem ETC. It is noteworthy that the inhibition of significant amounts of PSII centers by DCMU (up to $\alpha/\alpha_0 \approx 0.3$) caused only a moderate decrease in β/β_0. The convex-type plot of β/β_0

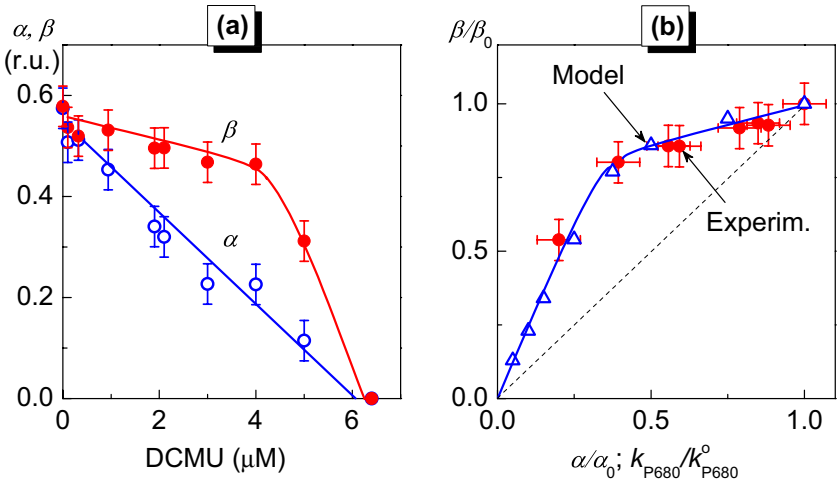

Fig. 3 *Panel a* experimental dependences of parameters α (*open circles*) and β (*closed circles*) on the concentration of DCMU (see notations in Fig. 2). *Panel b* the plot of β/β_0 versus α/α_0 (*solid circles* with *error bars*), where α_0 and β_0 stand for the corresponding parameters in control (untreated) chloroplasts, and its comparison with the theoretical dependence of β/β_0 versus the model parameter k_{P680}/k^0_{P680} computed for metabolic state 4, strong actinic light, and the relative capacity of the PQ pool $[PQ]_0/[P_{700}]_0 = 7$

versus α/α_0 (Fig. 3b) suggests that uninhibited PSII units were able to support efficient electron flow to P^+_{700}.

The ability of residual active PSII centers to keep a high level of electron flow from PSII to PSI can be explained by cooperation of PSII–LHCII complexes. It may occur because (1) photochemically active PSII units are able to donate electrons to the common pool of PQ molecules (Siggel et al. 1972; Tikhonov and Ruuge 1979; Haehnel 1982, 1984), and (2) due to the "excitonic" connectivity between the neighboring light-harvesting complexes of PSII. In the latter case, the light-harvesting pigments of DCMU-treated PSII–LHCII complexes retain the ability to "spill" excitation to adjacent PSII–LHCII units (for review, see Antal at al. 2013; Stirbet 2013). The electron current J^e_1 from PSI to the terminal acceptor (PSI → MV → O_2) depends on a number of active (reduced) P_{700} centers ($J^e_1 = L_1 \cdot k_{P700} \cdot [P_{700}]$), where L_1 stands for the number of light quanta exciting P_{700} per time unit, the coefficient k_{P700} characterizes the efficiency of P_{700} photooxidation, and $[P_{700}]$ is the relative concentration of reduced centers P_{700}. The convex-type plot of β/β_0 versus α/α_0 (Fig. 3b) suggests that the inhibition of a significant portion of PSII centers leads only to moderate attenuation of the overall electron flux through PSI.

Figure 4 schematically illustrates the scenarios of cooperation of PSII units via the common PQ pool. Note that PQ molecules present in significant surplus with respect to PSII, $([PQ] + [PQH_2])/[PSII] \sim 7$–10 (Stiehl and Witt 1969; Witt 1979). In control (untreated) chloroplasts, all active PSII units are involved in the reduction of the PQ pool (Fig. 4a). Siggel et al. (1972), who investigated the effectiveness of DCMU inhibitory action from the data on absorption changes of PQ and P_{700} in spinach chloroplasts, came to the conclusion about electron exchange between at least ten ETCs. Haehnel (1982) reported that the Cyt b_6f complex was able to donate electrons to more than ten PSI complexes. It is worthy of note that when significant amounts of PSII complexes are inhibited by DCMU, the residual uninhibited (photoactive) PSII units are still able to feed the PQ pool with electrons, thereby supporting interaction between spatially separated PSII and PSI complexes (Fig. 4b). In the latter case, the electron flow from PSII to PSI and further to O_2 (via MV) could be maintained at a high rate, provided the AL is strong enough for efficient feeding of P^+_{700} with electrons from the rest of active PSII complexes.

Note that the convex-type experimental dependence of β/β_0 versus α/α_0 coincides fairly well with the results of computer simulation of electron transport in thylakoids performed within the framework of our mathematical model (Fig. 3b, open triangles). Theoretical data presented in Fig. 3b are obtained for the model parameter $[PQ]_0 = 7$, which corresponds to 14 electron equivalents capable of accumulating in the reduced PQ pool. It should be stressed that this parameter coincides with the average capacity of the PQ pool ($[PQ]^{total}_0 \approx 7$) reported by Stiehl and Witt (1969) for spinach chloroplasts. Other details of our computer analysis of electron transport between PSII and PSI are considered below.

Modeling electron transport processes in chloroplasts

The conclusion about the role of the PQ pool as a common reservoir for electron equivalents, which supports an efficient functioning of the intersystem ETC upon modulation of PSII activity (either due to NPQ generation or due to inhibition of PSII reaction centers), finds a fairly good support from our computer model of electron and proton transport in chloroplasts.

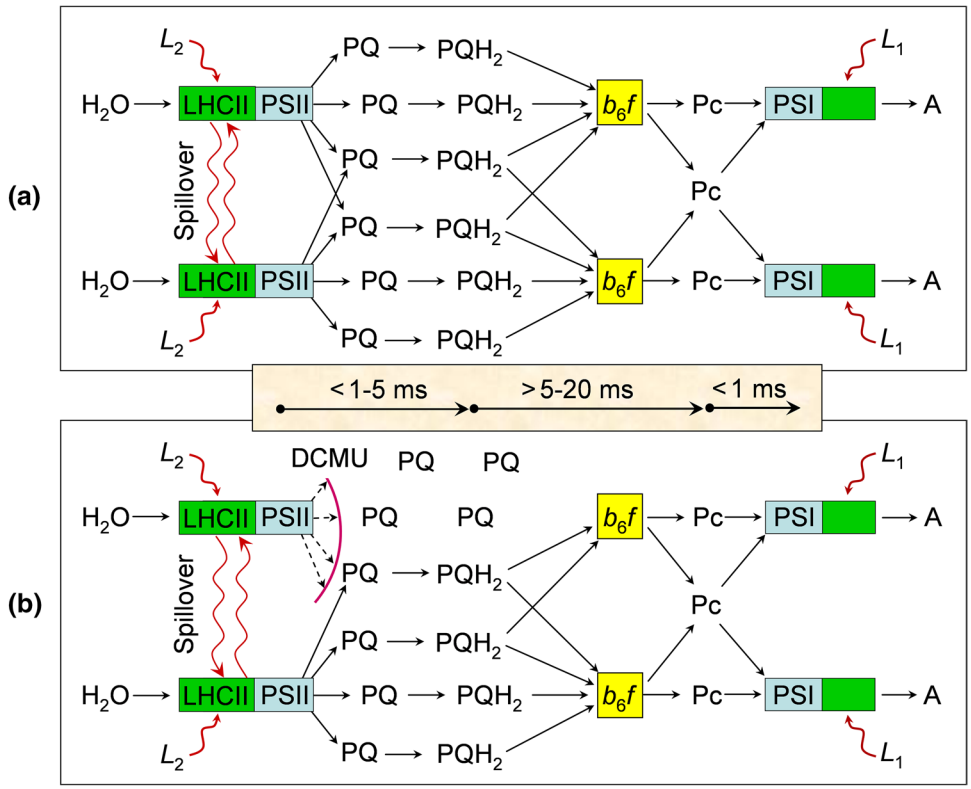

Fig. 4 A scheme illustrating cooperation of different PSII units via the common PQ pool and/or due to "excitonic" interactions between the light-harvesting pigments of PSII–LHCII complexes. *Panel a* control (untreated) chloroplasts; *panel b* chloroplasts in which some of the PSII complexes are inhibited by DCMU

Class B chloroplasts, water–water cycle

We start our analysis of electron transport in chloroplasts with the consideration of class B chloroplasts (thylakoids) in metabolic states 4 and 5 (classification according to Chance and Williams 1956), in which O_2 serves as the terminal electron acceptor and stromal pH_{out} = const (due to the presence of strong buffer). In isolated thylakoids, the physiological (PSI → CBC) and cyclic electron transport (around PSI) pathways do not operate, and the NPQ mechanism is inefficient. In the state of photosynthetic control (metabolic state 4), chloroplasts are able to generate the *trans*-thylakoid pH difference. For simulation of uncoupled chloroplasts (state 5), we assume that $pH_{in} = pH_{out}$.

Figure 5 presents the kinetics of redox transients of P_{700} and PQ induced by "Light 1" and after the change-over "Light 1 → Light 2" (the analog to chromatic transient $\lambda_{707} \rightarrow \lambda_{600}$), as well as the time-courses of pH_{in}. These kinetics were calculated for high AL (panels a–c) and low AL (panels d–f) for thylakoids in metabolic states 4 and 5. In both cases, similarly to experimental data, "Light 1" ($L_1/L_2 = 16$) induced the oxidation of all centers P_{700}. Switching "Light 1" to "Light 2" ($L_1/L_2 = 0.7$) caused a decrease in the level of P_{700}^+ due to electrons injected to the intersystem ETC from PSII. At strong "Light 2" (Fig. 5a), the pattern of P_{700}^+ transients depends on the metabolic state. In state 4, $[P_{700}^+]$ reached the steady-state level after the overshoot. The slow phase of the increase in $[P_{700}^+]$ (Fig. 5a) correlates with the rise of $[PQH_2]$ (Fig. 5b) caused by retardation to PQH_2 oxidation due to the light-induced acidification of the lumen (pH_{in} 5.3, Fig. 5c). Similarly to experimental data (Tikhonov et al. 1981), the overshoot in the kinetics of P_{700} transients is absent in uncoupled thylakoids ($pH_{in} = pH_{out} = 7.5$). In this case, the level of P_{700}^+ was somewhat lower and the relative number of reduced PQH_2 molecules was smaller than in state 4. At low AL, the above-mentioned difference between the patterns of redox transients of P_{700} and PQ in states 4 and 5 disappeared (Fig. 5d, e). This is because at low AL, the acidification of the lumen in state 4 was less significant (pH_{in} 6.5, Fig. 5f) than at high AL (pH_{in} 5.3, Fig. 5c). In both metabolic states, the level of reduced PQH_2 at low AL was significantly smaller than during the action of strong AL. This is because the rate of PQH_2 oxidation at pH_{in} 6.5 (low AL) is more rapid than at pH_{in} 5.3 (high AL).

As we noted above, the model allowed us to describe numerically experimental dependence β/β_0 versus α/α_0 (Fig. 3b). For modeling the inhibitory effect DCMU, we gradually reduced the model parameter k_{P680}, which determined the actuation frequency of PSII centers, keeping constant the model parameter k_{P700} characterizing the operation of PSI. The ratio k_{P680}/k_{P680}^0, where k_{P680}^0 stands for the initial value of the model parameter in control ("untreated") thylakoids and k_{P680} corresponds to reduced value of this

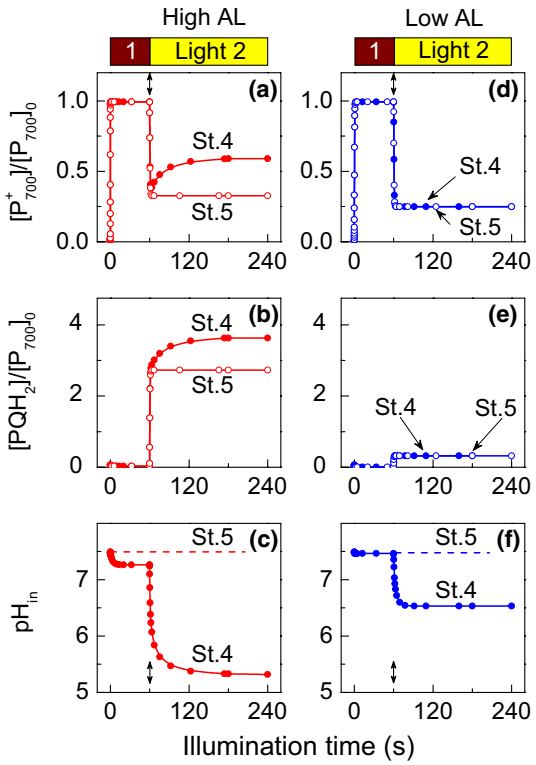

Fig. 5 Theoretical patterns of the light-induced redox transients of P_{700} (*panels a, d*) and PQ (*panels b, e*), and time-courses of the light-induced changes in pH_{in} (*panels c, f*) computed for two metabolic states of class B chloroplasts: state 4 (the state of photosynthetic control) and state 5 (uncoupled chloroplasts, $\Delta pH = 0$). *Panels a–c* correspond to high AL; *panels e–f* correspond to low AL. Here and below, $[P_{700}]_0$ is the total concentration of P_{700}

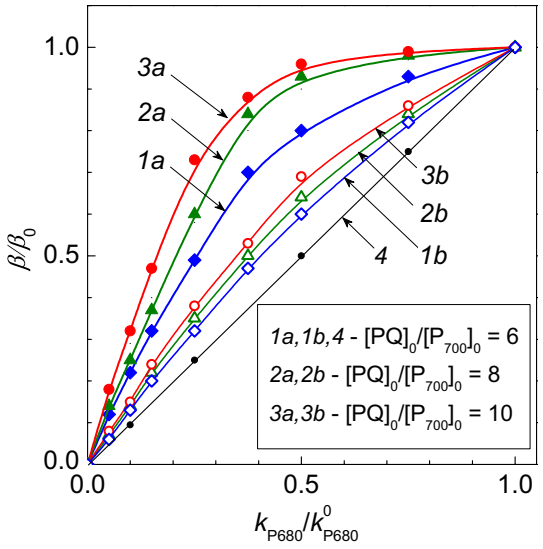

Fig. 6 Theoretical dependences of β/β_0 versus k_{P680}/k^0_{P680} for metabolic states 4 (*curves 1a, 2a, 3a, 4*) and 5 (*curves 1b, 2b, 3b*) calculated for different capacities of the PQ pool, as indicated. *Curves 1a, 1b, 2a, 2b, 3a*, and *3b* correspond to chloroplasts irradiated with "strong" light (HAL), *curve 4*—"weak" light (LAL)

parameter, simulates the inhibition of PSII by DCMU. Thus, the ratio k_{P680}/k^0_{P680} may be considered as the analog of experimentally determined ratio α/α_0. Figure 6 shows how variations of the PQ pool capacity ($[PQ]_0/[P_{700}]_0$ = 6, 8, and 10) affects the plot of β/β_0 versus k_{P680}/k^0_{P680}. As one can see, at strong AL, we obtained the convex-type plots of β/β_0 versus k_{P680}/k^0_{P680} similar to experimental dependence. Note that the bulge of the curve markedly increased with the rise of the PQ pool capacity. This result means that PQH_2 plays the role of the redox buffer. Accumulating electron equivalents in the ETC segment between PSII and PSI, PQH_2 molecules support efficient electron flow to PSI even upon the attenuated activity of PSII. Otherwise, the swelling of the curve becomes weaker in metabolic state 5 (Fig. 6, curves 1b, 2b, and 3b). Similar observation was reported by Siggel et al. (1972), who investigated the inhibition of electron transport in spinach chloroplasts by DCMU. The straightening of the curve β/β_0 versus k_{P680}/k^0_{P680} in state 5 can be easily explained by the release of the effect of pH_{in}-dependent deceleration of electron transfer from PQH_2 to the Cyt b_6f complex. Actually, in state 5, the steady-state concentration of PQH_2 decreases as compared to state 4 (Fig. 5b).

It should be noted that the convex-type patterns of dependences β/β_0 versus k_{P680}/k^0_{P680} are peculiar to sufficiently strong AL (Fig. 6, curves 1a, 2a, and 3a). With a decrease in the intensity of AL, the swelling of the dependence of β/β_0 versus k_{P680}/k^0_{P680} gradually disappears. For instance, there is the linear plot of β/β_0 versus k_{P680}/k^0_{P680} if the AL intensity is reduced by a factor of 10 (Fig. 6, curve 4). This can be accounted for by insignificant reduction of the PQ pool (compare panels b and e in Fig. 5).

Intact chloroplasts

Let us now consider the results of numerical experiments for intact chloroplasts, in which three alternative electron transport pathways on the acceptor side of PSI have been taken into account: (1) the outflow of electrons from PSI to $NADP^+$, (2) the WWC associated with the Mehler reaction (PSI → O_2), and (3) cyclic electron flow around PSI (Fig. 1). Computer experiments for "intact" chloroplasts demonstrated that the time-courses of the redox transients of P_{700} and PQ, as well as pH_{in}, were sensitive to AL intensity (Fig. 7). The steady-state level of P^+_{700} induced by "Light 2" decreased only insignificantly with the tenfold weakening of irradiation intensity. In the meantime, the redox status of the PQ pool was much more sensitive to attenuation of AL. At weak AL, the steady-state level of $[PQH_2]$ decreased by

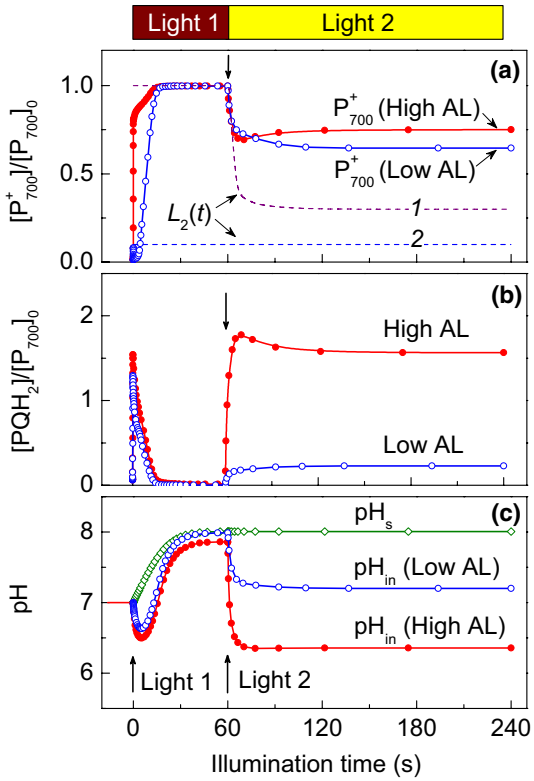

Fig. 7 Theoretical patterns of the light-induced redox transients of P_{700} (*panel a*), PQ (*panel b*), and changes in pH_{in} (*panel c*). Simulations were performed for intact chloroplasts in which operate three alternative pathways of electron transport (routes *1–3*) and the ATP synthase complexes

a factor of 7 as compared to strong AL. Also, there was the light-induced decrease in the value of $L_2(t)$ (Fig. 7a, curve 1) accounted for by the lumen acidification (pH_{in} 6.4). From the phenomenological point of view, the light-induced decrease in $L_2(t)$ is similar to attenuation of PSII activity due to the light-induced generation of NPQ. At low AL, $L_2(t) = \text{const}$ (Fig. 7a, curve 2) because the internal pH_{in} 7.2 (Fig. 7c) is insufficient to slow down the oxidation of PQH_2. Variations of the AL intensity led to modulation of the redox status of the PQ pool: $[PQH_2]$ decreases significantly with the attenuation of AL (Fig. 7b).

Summarizing the results of computer experiments, we can conclude that the nonlinear response of P_{700} to variations of PSII activity, which manifests itself at high intensities of AL, reflects the "electronic communication" between different ETCs through the common pool of PQ molecules. The PQH_2 pool serves as the "buffer" accumulating electron equivalents injected into the intersystem ETC by PSII, thereby providing efficient electron flow from PSII to PSI upon fluctuations of ambient light.

Concluding remarks

The capability of plants to develop NPQ depends on their growth conditions (for review, see Demmig-Adams et al. 2012). The long-term acclimation of plants to HL irradiation promotes the expression of the regulatory protein PsbS, which is responsible for rapid enhancement of NPQ (pH_{in}-dependent component of NPQ, qE), protecting PSII from photoinhibition (Li et al. 2002, 2004). Under solar stress conditions, the expression of PsbS increases (Ikeuchi et al. 2014; Dong et al. 2015; Ware et al. 2015b). The comparative study of two contrasting species of *Tradescantia* (sun- and shade-tolerant species *Tradescantia sillamontana* and *Tradescantia fluminensis*) revealed that HL-grown plants of both species showed higher levels of the PsbS protein and correlated with increased capacity of plants for generation of high NPQ at strong AL (Mishanin et al. 2016). In the meantime, the steady-state levels of P^+_{700} induced by strong AL were virtually the same in the LL- and HL-grown plants of both species (Mishanin et al. 2017). The latter result suggests that the ratio of the apparent rate constants of the electron drain from PSI (k_1) and the electron influx to P^+_{700} (k_2) remained invariant, $k_1/k_2 \approx \text{const}$, regardless of the growth conditions. Due to "electronic" and "excitonic" connectivity of PSII units, the overall flux of electrons to PSI may be maintained at a high level even in the course of NPQ development. This is because the rate-limiting step of the intersystem electron transport is beyond the stage of PQH_2 formation in PSII. Thus, the common denominator of our previous and current studies is that at strong AL the attenuation of PSII activity, either by direct inhibition of PSII or due to the enhancement of NPQ, may not cause dramatic reduction of the electron flow through PSI. Feeding the PQ pool with electrons donated by PSII will help to maintain efficient electron flow to P^+_{700} even during the NPQ-dependent decrease in PSII activity. Results of our computer simulations are in a fair agreement with experimental data. This conclusion can be appreciated in the context of the NPQ-dependent mechanism of photoprotection in plants: generation of NPQ helps to avoid solar stress due to dissipation of excess energy in PSII, while the overall rate of electron flow through PSI would not decrease dramatically, supporting efficient photosynthetic performance.

Appendix

Let us consider the kinetics of P_{700} re-oxidation during the action of the far-red light (λ_{707}).

Suppose that Q_0 is a number of electron equivalents accumulated in the intersystem ETC during preliminary illumination of chloroplasts by "Light 2" exciting both

photosystems. The pool of reduced electron carrier serves as the "reservoir" of electrons donated to P_{700}^{+} during illumination of chloroplasts by the far-red λ_{707} of intensity J_{707}. If the outflow of electrons from PSI does not limit the actuation of P_{700} centers, we can evaluate the rate of electron flow J_1^e from PSI to O_2 using the following approximation:

$$J_1^e = L_1 \cdot k_{P700} \cdot [P_{700}], \quad (1)$$

where L_1 is the number of light quanta exciting P_{700} per time unit and the coefficient k_{P700} characterizes the efficiency of P_{700} photooxidation. In this case, we can write the trivial relationship (Eq. 2), which connects the electron capacity Q_0 of the reduced pool of the intersystem electron carriers, on the one hand, and the so-called "work integral" W determined from the kinetics of P_{700} re-oxidation, on the other hand:

$$Q_0 = \int_0^\infty L_1 k_{P700}[P_{700}]dt = L_1 k_{P700} S \equiv L_1 \cdot W. \quad (2)$$

The so-called "work integral" $W = k_{P700}S$ is proportional to the area S over the kinetic curve for P_{700} re-oxidation during the action of the far-red light (for definition of S, see Fig. 2). It is noteworthy that the relationship $Q_0 = L_1 \cdot W$ should hold true at various intensities of the actinic light L_1 only if the efflux of electrons from PSI does not limit the overall rate of electron flow.

Figure 8 shows the plots of the product $J_{707} \cdot S$ versus J_{707} obtained for aerated suspension of bean chloroplasts. The values J_{707} are proportional to the intensity of the far-red light λ_{707} which induced the re-oxidation of P_{700} after pre-illumination (30 s) of chloroplasts with the orange light

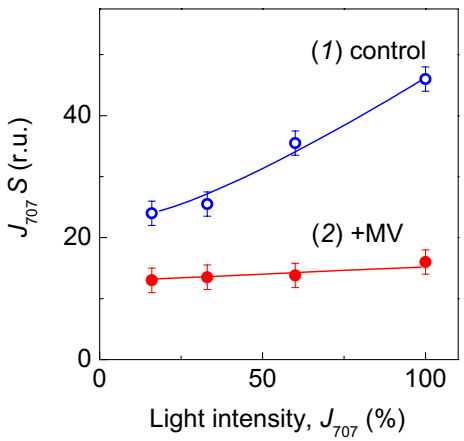

Fig. 8 The plots of the product $J_{707} \cdot S$ versus the intensity J_{707} of the far-red light λ_{707} measured for class B chloroplasts. *Curve 1* chloroplasts without added MV, *curve 2* chloroplasts in the presence of 2 μM MV. 100% of J_{707} corresponds to 75 μmol m^{-2} s^{-1}. For more details, see text

λ_{600}. In the lack of MV (control chloroplasts), the product $J_{707} \cdot S$ increases with the rise of J_{707} (Fig. 7, curve 1). This indicates that the efflux of electrons from PSI to O_2 is somewhat hampered. Otherwise, in the presence of catalytic amounts of MV (2 μM), the product $J_{707} \cdot S$ is independent of J_{707} (Fig. 7, curve 2). The fact that the relationship $J_{707} \cdot S = \text{const}$ holds true at different intensities of the far-red light J_{707} suggests that MV mediates rapid electron transfer from PSI to O_2, thereby releasing the impediment to O_2-dependent autooxidation of electron carriers on the acceptor side of PSI.

Acknowledgements This work was supported in part by the Russian Foundation for Basic Research (RFBR Project 15-04-03790a). We also thank the anonymous reviewers for their valuable comments.

References

Allakhverdiev SI, Murata N (2004) Environmental stress inhibits the synthesis de novo of proteins involved in the photodamage–repair cycle of photosystem II in *Synechocystis* sp. PCC 6803. Biochim Biophys Acta 1657:23–32

Allen JF (1992) Protein phosphorylation in regulation of photosynthesis. Biochim Biophys Acta 1098:275–335

Antal TK, Kolacheva A, Maslakov A, Riznichenko GYu, Krendeleva TE, Rubin AB (2013) Study of the effect of reducing conditions on the initial chlorophyll fluorescence rise in the green microalgae *Chlamydomonas reinhardtii*. Photosynth Res 114:143–154

Asada K (1999) The water-water cycle in chloroplasts: scavenging of active oxygens and dissipation of excess photons. Annu Rev Plant Physiol Plant Mol Biol 50:601–639

Ballottari M, Dall'Osto L, Morosinotto T, Bassi R (2007) Contrasting behavior of higher plant photosystem I and II antenna systems during acclimation. J Biol Chem 282:8947–8958

Balsera M, Schürmann P, Buchanan BB (2016) Redox regulation in chloroplasts. In: Kirchhoff H (ed) Chloroplasts. Current research and future trends, Caister Academic Press, Poole, pp. 187–207

Blankenship RE (2002) Molecular mechanisms of photosynthesis. Blackwell, Oxford

Boichenko VA (1998) Action spectra and functional antenna sizes of photosystems I and II in relation to the thylakoid membrane organization and pigment composition. Photosynth Res 58:163–174

Cardona T, Sedoud A, Cox N, Rutherford AW (2012) Charge separation in photosystem II: a comparative and evolutionary overview. Biochim Biophys Acta 1817:26–43

Chance B, Williams GR (1956) The respiratory chain and oxidative phosphorylation. Adv Enzymol 17:65–134

Demmig-Adams B (1990) Carotenoids and photoprotection in plants: a role of xanthophyll zeaxanthin. Biochim Biophys Acta 1020:1–24

Demmig-Adams B, Cohu CM, Muller O, Adams WW (2012) Modulation of photosynthetic energy conversion efficiency in nature: from seconds to seasons. Photosynth Res 113:75–88

Dong L, Tua W, Kun Liu, Sun R, Liu C, Wang K, Yang C (2015) The PsbS protein plays important roles in photosystem II supercomplex remodeling under elevated light conditions. J Plant Physiol 172:33–41

Eberhard S, Finazzi G, Wollman FA (2008) The dynamics of photosynthesis. Annu Rev Genet 42:463–515

Edwards GE, Walker DA (1983) C3, C4: mechanisms, and cellular and environmental regulation of photosynthesis. Blackwell, Oxford

Haehnel W (1976) The reduction kinetics of chlorophyll a_1 as an indicator of for proton uptake between the light reactions in chloroplasts. Biochim Biophys Acta 440:506–521

Haehnel W (1982) On the functional organization of electron transport from plastoquinone to photosystem I. Biochim Biophys Acta 682:245–247

Haehnel W (1984) Photosynthetic electron transport in higher plants. Annu Rev Plant Physiol 35:659–693

Horton P (2012) Optimization of light harvesting and photoprotection: molecular mechanisms and physiological consequences. Phil Trans R Soc B 367:3455–3465

Ikeuchi M, Uebayashi N, Sato F, Endo T (2014) Physiological functions of PsbS-dependent and PsbS-independent NPQ under naturally fluctuating light conditions. Plant Cell Physiol 55:1286–1295

Jahns P, Holzwarth AR (2012) The role of the xanthophylls cycle and of lutein in photoprotection of photosystem II. Biochim Biophys Acta 1817:182–193

Jallet D, Cantrell M, Peers G (2016) New players for photoprotection and light acclimation. In: Kirchhoff H (ed) Chloroplasts. Current research and future trends, Caister Academic Press, Poole, pp. 135–159

Johnson MP, Goral TK, Duffy CDP, Brain APP, Mullineaux CP, Ruban AV (2011) Photoprotective energy dissipation involves the reorganization of photosystem II light-harvesting complexes in the grana membranes of spinach chloroplasts. Plant Cell 23:1468–1479

Junge W, Nelson N (2015) ATP synthase. Annu Rev Biochem 83:631–657

Kozuleva MA, Petrova AA, Mamedov MD, Semenov AY, Ivanov BN (2014) O_2 reduction by photosystem I involves phylloquinone under steady-state illumination. FEBS Lett 588:4364–4368

Kuvykin IV, Vershubskii AV, Priklonskii VI, Tikhonov AN (2009) Computer simulation study of pH-dependent regulation of electron transport in chloroplasts. Biophysics 54:455–464

Kuvykin IV, Ptushenko VV, Vershubskii AV, Tikhonov AN (2011) Regulation of electron transport in C_3 plant chloroplasts in situ and in silico. Short-term effects of atmospheric CO_2 and O_2. Biochim Biophys Acta 1807:336–347

Laisk A, Oja V, Eichelmann H, Dall'Osto L (2014) Action spectra of photosystems II and I and quantum yield of photosynthesis in leaves in State 1. Biochim Biophys Acta 1837:315–325

Lemeille S, Rochaix J-D (2010) State transitions at the crossroad of thylakoid signaling pathways. Photosynth Res 106:33–46

Li X-P, Björkman O, Shih C, Grossmann AR, Rosenquist M, Jansson S, Niyogi KK (2000) A pigment-binding protein essential for regulation of photosynthetic light harvesting. Nature 403:391–395

Li X-P, Muller-Moule P, Gilmore AM, Niyogi KK (2002) PsbS dependent enhancement of feedback de-excitation protects photosystem II from photoinhibition. Proc Natl Acad Sci USA 99:15222–15227

Li X-P, Gilmore AM, Caffarri S, Bassi R, Golan T, Kramer D, Niyogi KK (2004) Regulation of photosynthetic light harvesting involves intrathylakoid lumen pH sensing by the PsbS protein. J Biol Chem 279:22866–22874

Li Z, Wakao S, Fischer BB, Niyogi KK (2009) Sensing and responding to excess light. Annu Rev Plant Biol 60:239–260

Mamedov M, Govindjee, Nadtochenko V, Semenov A (2015) Primary electron transfer processes in photosynthetic reaction centers from oxygenic organisms. Photosynth Res 125:51–63

Matsubara S, Förster B, Waterman M, Robinson SA, Pogson BJ, Gunning B, Osmond B (2012) From ecophysiology to phenomics: some implications of photoprotection and shade–sun acclimation in situ for dynamics of thylakoids in vitro. Phil Trans R Soc B 367:3503–3514

Mehler AH (1951) Studies on reactions of illuminated chloroplasts. I. Mechanisms of the reduction of oxygen and other Hill reagents. Arch Biochem Biophys 33:65–77

Michelet L, Zaffagnini M, Morisse S, Sparla F, Perez-Perez ME, Francia F, Danon A, Marchand CH, Fermani S, Trost P, Lemaire SD (2013) Redox regulation of the Calvin–Benson cycle: something old, something new. Front Plant Sci. doi:10.3389/fpls.2013.00470

Mishanin VI, Trubitsin BV, Benkov MA, Minin AA, Tikhonov AN (2016) Light acclimation of shade-tolerant and light-resistant *Tradescantia* species: induction of chlorophyll *a* fluorescence and P_{700} photooxidation, expression of *PsbS* and *Lhcb1* proteins. Photosynth Res 130:275–291

Mishanin VI, Trubitsin BV, Patsaeva SV, Ptushenko VV, Solovchenko AE, Tikhonov AN (2017) Acclimation of shade-tolerant and light-resistant *Tradescantia* species to growth light: chlorophyll *a* fluorescence, electron transport, and xanthophylls content. Photosynth Res. doi:10.1007/s11120-017-0339-1

Mitchell P (1966) Chemiosmotic coupling in oxidative and photosynthetic phosphorylation. Biol Rev 41:445–502

Miyake C (2010) Alternative electron flows (water-water cycle and cyclic electron flow around PSI) in photosynthesis: molecular mechanisms and physiological functions. Plant Cell Physiol 51:1951–1963

Murata N, Allakhverdiev SI, Nishiyama Y (2012) The mechanism of photoinhibition in vivo: re-evaluation of the roles of catalase, α-tocopherol, nonphotochemical quenching, and electron transport. Biochim Biophys Acta 1817:1127–1133

Nelson DL, Cox MM (2012) Lehninger principles of biochemistry, 6th edn. Freeman, W. H. & Company, New York

Ocampo-Alvarez H, Garcia-Mendoza E, Govindjee (2013) Antagonist effect between violaxanthin and de-epoxidated pigments in non-photochemical quenching induction in the qE deficient brown alga *Macrocystis pyrifera*. Biochim Biophys Acta 1827:427–437

Puthiyaveetil S, Kirchhoff H, Höhner R (2016) Structural and Functional Dynamics of the Thylakoid Membrane System. In: Kirchhoff H (ed) Chloroplasts. Current research and future trends, Caister Academic Press, Poole, pp. 59–87

Rochaix J-D (2014) Regulation and dynamics of the light-harvesting system. Annu Rev Plant Biol 65:287–309

Ruban A (2012) The photosynthetic membrane: molecular mechanisms and biophysics of light harvesting. Wiley, Oxford

Ruban AV, Johnson MP, Dufy CDP (2012) The photoprotective molecular switch in the photosystem II antenna. Biochim Biophys Acta 1817:167–181

Rubin A, Riznichenko G (2014) Mathematical biophysics. Series: biological and medical physics, biomedical engineering. Springer, New York

Rutherford AW, Crofts AR, Inoue Y (1982) Thermoluminescence as a probe of photosystem II photochemistry. The origin of the flash-induced glow peaks. Biochim Biophys Acta 682:457–465

Schmitt F-J, Renger G, Friedrich T, Kreslavski VD, Zharmukhamedov SK, Los DA, KuznetsovVV, Allakhverdiev SI (2014) Reactive oxygen species: Re-evaluation of generation, monitoring and role in stress-signaling in phototrophic organisms. Biochim Biophys Acta 1837:835–848

Siggel U, Renger G, Stiehl HH, Rumberg B (1972) Evidence for electronic and ionic interaction between electron transport chains in chloroplasts. Biochim Biophys Acta 256:328–335

Stiehl HH, Witt HT (1969) Quantitative treatment of the function of plastoquinone in photosynthesis. Z Naturforsch 24b:1588–1598

Stirbet A (2013) Excitonic connectivity between photosystem II units: what is it, and how to measure it. Photosynth Res 116:189–214

Strand DD, Fisher N, Kramer DM (2016) Distinct energetics and regulatory functions of the two major cyclic electron flow pathways in chloroplasts. In: Kirchhoff H (ed) Chloroplasts. Current research and future trends, Caister Academic Press, Poole, pp. 89–100

Tikhonov AN (2013) pH-Dependent regulation of electron transport and ATP synthesis in chloroplasts. Photosynth Res 116:511–534

Tikhonov AN (2014) The cytochrome b_6f complex at the crossroad of photosynthetic electron transport pathways. Plant Physiol Biochem 81:163–183

Tikhonov AN (2015) Induction events and short-term regulation of electron transport in chloroplasts: an overview. Photosynth Res 125:65–94

Tikhonov AN (2016) Modeling electron and proton transport in chloroplasts. In: Kirchhoff H (ed) Chloroplasts. Current research and future trends, Caister Academic Press, Poole, pp. 101–134

Tikhonov AN, Ruuge EK (1979) Electron paramagnetic resonance study of electron transport in photosynthetic systems. VIII. The interplay between two photosystems and kinetics of P700 redox transients under various conditions of flash excitation. Molec Biol 13:1085–1097

Tikhonov AN, Vershubskii AV (2014) Computer modeling of electron and proton transport in chloroplasts. Biosystems 121:1–21

Tikhonov AN, Khomutov GB, Ruuge EK, Blumenfeld LA (1981) Electron transport control in chloroplasts. Effects of photosynthetic control monitored by the intrathylakoid pH. Biochim Biophys Acta 637:321–333

Tikkanen M, Aro E-M (2012) Thylakoid protein phosphorylation in dynamic regulation of photosystem II in higher plants. Biochim Biophys Acta 1817:232–238

Tikkanen M, Aro E-M (2014) Integrative regulatory network of plant thylakoid energy transduction. Trends Plant Sci 19:10–17

Tikkanen M, Grieco M, Nurmi M, Rantala M, Suorsa M, Aro E-M (2012) Regulation of the photosynthetic apparatus under fluctuating growth light. Philos Trans R Soc Lond B 367:3486–3493

Trubitsin BV, Mamedov MD, Semenov AYu, Tikhonov AN (2014) Interaction of ascorbate with photosystem I. Photosynth Res 122:215–231

Trubitsin BV, Vershubskii AV, Priklonskii VI, Tikhonov AN (2015) Short-term regulation and alternative pathways of photosynthetic electron transport in *Hibiscus rosa-sinensis* leaves. J Photochem Photobiol B 152:400–415

Vershubskii AV, Priklonskii VI, Tikhonov AN (2001) Electron and proton transport in chloroplasts: a mathematical model constructed with regard for the lateral heterogeneity of thylakoids. Biophysics 46:448–457

Vershubskii AV, Priklonskii VI, Tikhonov AN (2004) Effects of diffusion and topological factors on the efficiency of energy coupling in chloroplasts with heterogeneous partitioning of protein complexes in thylakoids of grana and stroma. A mathematical model. Biochemistry 69:1016–1024

Vershubskii AV, Kuvykin IV, Priklonskii VI, Tikhonov AN (2011) Functional and topological aspects of pH-dependent regulation of electron and proton transport in chloroplasts in silico. BioSystems 103:164–179

Vershubskii AV, Trubitsin BV, Priklonskii VI, Tikhonov AN (2017) Lateral heterogeneity of the proton potential along the thylakoid membranes of chloroplasts. Biochim Biophys Acta 1859:388–401

Ware MA, Belgio E, Ruban AV (2015a) Photoprotective capacity of nonphotochemical quenching in plants acclimated to different light intensities. Photosynth Res 126:261–274

Ware MA, Giovagnetti V, Belgio E, Ruban AV (2015b) PsbS protein modulates non-photochemical chlorophyll fluorescence quenching in membranes depleted of photosystems. J Photochem Photobiol B 152:301–307

Webber AN, Lubitz W (2001) P700: the primary electron donor of photosystem I. Biochim Biophys Acta 1507:61–79

Witt HT (1979) Energy conversion in the functional membrane of photosynthesis. Analysis by light pulse and electric pulse methods. Biochim Biophys Acta 505:355–427

Yamamoto Y, Yoshioka-Nishimura M (2016) Photoinhibition and the damage repair cycle of photosystem II. In: Kirchhoff H (ed) Chloroplasts. Current research and future trends, Caister Academic Press, Poole, pp. 161–170